Finite element solution of hyperbolic equations I.One-dimensional case

Vittorio Selmin

INRIA

UNITÉ DE RECHERCHE
INRIA-SOPHIA ANTIPOLIS

Institut National
de Recherche
en Informatique
et en Automatique

Domaine de Voluceau
Rocquencourt
B.P.105
78153 Le Chesnay Cedex
France

Tél. (1) 39.63.55.11

Rapports de Recherche

N° 655

FINITE ELEMENT SOLUTION OF HYPERBOLIC EQUATIONS

I.

ONE-DIMENSIONAL CASE

Vittorio SELMIN

Avril 1987

FINITE ELEMENT SOLUTION OF HYPERBOLIC EQUATIONS I. ONE DIMENSIONAL CASE

RESOLUTION D'EQUATIONS HYPERBOLIQUES PAR UNE METHODE D'ELEMENTS FINIS I. LE CAS MONODIMENSIONNEL

Vittorio SELMIN

INRIA Sophia-Antipolis
Avenue Emile Hughes
(Anc. Route des Lucioles)
Sophia Antipolis
06565 VALBONNE

Abstract

We compare a number of methods which try to combine the advantages of a monotone scheme, which produces no "ripples" near discontinuities, together with those of a second-order one. This two schemes are formulated within the framework of the Taylor-Galerkin finite element method. We have tested artificial viscosity methods, TVD methods and FCT methods. Numerical results for the one-dimensional shock tube problem are presented.

Résumé

On compare différentes méthodes qui essayent de combiner les avantages d'un schéma monotone, qui ne produit pas d'oscillations près des discontinuités, avec ceux d'un schéma précis au second ordre. Ces deux schémas sont construits en utilisant la méthode Taylor-Galerkin des éléments finis. On a testé des méthodes de viscosité artificielle, des méthodes TVD et des méthodes FCT. Des exemples numériques concernant la résolution du problème du tube à choc monodimensionnel sont présentés.

Contents

I. Introduction

It is well known that second-order or higher order schemes for the numerical solution of nonlinear hyperbolic problems, such as the Euler equations, suffer from dispersive "ripples" in the computed solutions, particularly near steep gradients. Schemes of lower accuracy or schemes with zero-order diffusion added locally produce no ripples but tend to suffer from excessive numerical diffusion. This report describes and compares a number of methods which try to combine the advantages of both approaches. In section II we discuss first- and second-order schemes formulated within the framework of the finite element methods of Taylor-Galerkin type[1]; then, in section III,IV and V we describe and illustrate the artificial viscosity method[2,3], the Total Variation Diminishing (TVD) concept[4,5] and the Flux Corrected Transport(FCT) technique[6], respectively.

The different methods are used to integrate the one-dimensional equations of gas dynamics for an inviscid, non heat conducting fluid, i.e. the Euler equations. These equations are written in conservative form as

$$\frac{\partial U}{\partial t} + \frac{\partial F(U)}{\partial x} = 0 \quad , \tag{1}$$

where

$$U = \begin{pmatrix} \rho \\ m \\ e \end{pmatrix} \ , \ F = \begin{pmatrix} m \\ m^2/\rho + p \\ (e+p)m/\rho \end{pmatrix} \quad .$$

Here U is the vector of conservative variables, F is the flux vector and $m = \rho v$ is the momentum density. The primitive variables are the density ρ , the velocity v and the pressure p.
The total energy per unit volume e is defined for a polytropic gas as

$$e = \frac{p}{\gamma - 1} + \frac{m^2}{2\rho}$$

where γ is the ratio of specific heats ($\gamma = 1.4$ for air).
Let A denote the Jacobian matrix $\partial F(U)/\partial U$ whose eigenvalues are

$$(a^1, a^2, a^3) = (v - c, v, v + c)$$

where $c = \sqrt{\gamma p/\rho}$ is the speed of sound. The right eigenvectors of A form the matrix T given by

$$T = \begin{pmatrix} 1 & 1 & 1 \\ v-c & v & v+c \\ h-vc & \frac{1}{2}v^2 & h+vc \end{pmatrix}$$

where the enthalpy per unit mass h is defined by

$$h = \frac{c^2}{\gamma - 1} + \frac{v^2}{2}$$

The matrix T is invertible and diagonalizes A , namely

$$T^{-1}AT = \Lambda \; ; \; \Lambda_{ij} = a^i \delta_{ij}$$

Note that Eq.(1) can be rewritten in characteristic form

$$T^{-1}\frac{\partial U}{\partial t} + \Lambda T^{-1}\frac{\partial U}{\partial x} = 0$$

We will present numerical results for the shock tube problem used by Sod [7] to compare the most popular numerical methods. In this one-dimensional problem, an initial discontinuity in the thermodynamical state of the gas(Riemann problem) breaks into a shock wave followed by a contact discontinuity and a rarefaction wave. All the variables are discontinuous across a shock wave whereas, across a contact discontinuity, the density is discontinuous but the pressure and the velocity are continuous. On the contrary, in the rarefaction wave all the variables are continuous. The initial condition at $t = 0$ is specified by the data

$$\begin{cases} \rho = 1.000 \; ; \; v = 0.00 \; ; \; p = 1.00 & 0 \leq x \leq \frac{1}{2} \\ \rho = 0.125 \; ; \; v = 0.00 \; ; \; p = 0.10 & \frac{1}{2} < x \leq 1 \end{cases} \tag{2}$$

The numerical calculations are shown at $t = 0.2$ and compared with the analytical solution. In all calculations 101 mesh points have been used with a CFL number equal to 0.55, 0.733 or 0.916 depending on the numerical stability of the schemes (see later).

II. First- and second-order finite element schemes

Consider a nonlinear but scalar conservation law in one dimensional space

$$\frac{\partial u}{\partial t} + \frac{\partial f(u)}{\partial x} = 0 \tag{3}$$

The approximate solution of Eq.(3) at the point (x_j, t^n) with $x_j = jh$ and $t^n = n\Delta t$ will be denoted by u_j^n, where h and Δt are increments in space and in time, respectively.

1. Second-order scheme

The Eq.(3) is discretized in time as in the classical Lax-Wendroff scheme [8] or in the Taylor-Galerkin scheme of second-order accuracy in time[9] :

$$\frac{u^{n+1} - u^n}{\Delta t} = -\frac{\partial f^n}{\partial x} + \frac{\Delta t}{2}\frac{\partial}{\partial x}(a^n \frac{\partial f^n}{\partial x}) \tag{4}$$

where $u^n = u(x, t^n)$, $f^n = f(u^n)$ and $a^n = a(u^n) = \partial f(u^n)/\partial u$.
To introduce a spatial approximation by means of the finite element method, Eq(4) must be recast in a weak form in accordance to the standard weighted residual formulation which gives :

$$< w, \frac{u^{n+1} - u^n}{\Delta t} > = < \frac{\partial w}{\partial x}, f^n > - \frac{\Delta t}{2} < a^n \frac{\partial w}{\partial x}, \frac{\partial f^n}{\partial x} > + \textit{boundary terms} \tag{5}$$

where $< u, v >$ denotes the L^2-inner product $\int uvdx$ over the domain of the problem and w is a suitable weighting function.
The spatial approximation of Eq.(5) is performed according to the standard Galerkin finite element method. The unknown u and the weighting function w are taken in the same space and are approximated locally by means of piecewise linear functions. The equation thus obtained at node j can be written in the form

$$[1 + \frac{1}{6}(\Delta_{j+\frac{1}{2}} - \Delta_{j-\frac{1}{2}})]u_j^{n+1} = [1 + \frac{1}{6}(\Delta_{j+\frac{1}{2}} - \Delta_{j-\frac{1}{2}})]u_j^n + \lambda(G_{j+\frac{1}{2}}^n - G_{j-\frac{1}{2}}^n) \tag{6}$$

where

$$G_{j+\frac{1}{2}} = f_{j+\frac{1}{2}} - \frac{\lambda}{2} a^2_{j+\frac{1}{2}} \Delta_{j+\frac{1}{2}} u_j \ ,$$

$$\Delta_{j+\frac{1}{2}} u_j = u_{j+1} - u_j \ , \ \lambda = \frac{\Delta t}{h}$$

and $f_{j+\frac{1}{2}}$ is a convenient average of $f_{j+1} \equiv f(u_{j+1})$ and $f_j \equiv f(u_j)$. When the flux f is linearly interpolated ; $f_{j+\frac{1}{2}}$ takes the form

$$f_{j+\frac{1}{2}} = \frac{1}{2}(f_j + f_{j+1})$$

These characterizations of the advection term give identical expressions in the case of a linear equation whereas their difference is $\theta(h^2)$ in the nonlinear case[10].

2. First-order scheme

If the consistent mass operator is diagonalized, i.e. if one introduces the approximation

$$1 + \frac{1}{6}[\Delta_{j+\frac{1}{2}} - \Delta_{j-\frac{1}{2}}] \to 1$$

in the left-hand side of Eq.(6) (but not in the right-hand side), the following first-order accurate scheme is obtained

$$u_j^{n+1} = u_j^n - \lambda(H^n_{j+\frac{1}{2}} - H^n_{j-\frac{1}{2}}) \tag{7}$$

where $\lambda H_{j+\frac{1}{2}} = \lambda f_{j+\frac{1}{2}} - \frac{1}{2}(\lambda^2 a^2_{j+\frac{1}{2}} + \frac{1}{3})\Delta_{j+\frac{1}{2}} u_j$.
This scheme can be interpreted as a second-order approximation of the parabolic equation

$$\frac{\partial u}{\partial t} + \frac{\partial f}{\partial x} = \frac{h^2}{6\Delta t} \frac{\partial^2 u}{\partial x^2}$$

It has the following domain of numerical stability :

$$|\nu| \leq \sqrt{\frac{2}{3}}$$

where $\nu = \lambda a$ is the Courant number. In this whole range, it is monotone[11] and satisfies the entropy condition. Consequently, the solution of scheme(7) converges to the physically relevant solution of Eq.(3), which is not always true for second-order schemes.

The first-order scheme can also be implemented by means of a splitting-up procedure. In fact, Eq.(7) is equivalent to the following two-step scheme :

$$\begin{cases} [1+\frac{1}{6}(\Delta_{j+\frac{1}{2}}-\Delta_{j-\frac{1}{2}})](u_j^{n+\frac{1}{2}}-u_j^n)=-\lambda(G^n_{j+\frac{1}{2}}-G^n_{j-\frac{1}{2}}) \\ u_j^{n+1}=u_j^{n+\frac{1}{2}}+\frac{1}{6}(\Delta_{j+\frac{1}{2}}-\Delta_{j-\frac{1}{2}})u_j^{n+\frac{1}{2}} \end{cases} \tag{8}$$

Notice that the diffusion step introduces only a real multiplicative coefficient into the amplification factor as compared to that associated to Eq.(6) and does not disturb the phases.

3. First-order scheme with modulated dissipation

The dissipation term of the monotone scheme can be modulated by introducing a parameter d, $0 \leq d \leq 1$. Two different schemes are obtained depending on whether the one-step or two-step form of the monotone scheme is started from .

3.1. *One-step scheme with modulated dissipation*

$$u_j^{n+1}=u_j^n-\lambda[H^n_{j+\frac{1}{2}}(d)-H^n_{j-\frac{1}{2}}(d)] \tag{9}$$

where $\lambda H_{j+\frac{1}{2}}(d)=\lambda f_{j+\frac{1}{2}}-\frac{1}{2}(\lambda^2 a^2_{j+\frac{1}{2}}+\frac{d_{j+\frac{1}{2}}}{3})\Delta_{j+\frac{1}{2}}u_j$. In the case $d=0$, we obtain a Lax-Wendroff type scheme[8]. The condition of stability is $\nu^2 \leq 1-\frac{d}{3}$.

3.2. *Two-step scheme with modulated dissipation*

$$\begin{cases} [1+\frac{1}{6}(\Delta_{j+\frac{1}{2}}-\Delta_{j-\frac{1}{2}})](u_j^{n+\frac{1}{2}}-u_j^n)=-\lambda(G^n_{j+\frac{1}{2}}-G^n_{j-\frac{1}{2}}) \\ u_j^{n+1}=u_j^{n+\frac{1}{2}}+\frac{1}{6}(d_{j+\frac{1}{2}}\Delta_{j+\frac{1}{2}}-d_{j-\frac{1}{2}}\Delta_{j-\frac{1}{2}})u_j^{n+\frac{1}{2}} \end{cases} \tag{10}$$

In the case $d=0$, scheme(8)' is obtained. The stability condition for this scheme is complicated and can be approximated, in the range $0 \leq d \leq 1$, by

$$\nu^2 \leq \frac{1}{\sqrt{3}}[1+d(\sqrt{2}-1)]$$

For the last two schemes, it can be useful to introduce the artificial viscosity operator

$$D_j u_j=(D_{j+\frac{1}{2}}-D_{j-\frac{1}{2}})u_j \tag{11}$$

where

$$D_{j+\frac{1}{2}}u_j=\frac{d_{j+\frac{1}{2}}}{6}\Delta_{j+\frac{1}{2}}u_j \tag{12}$$

III. Artificial viscosity method

As shown in Fig.(1), the solution obtained with second-order schemes suffers from dispersive "ripples" particularly near discontinuities whereas the first-order scheme produces no ripples but suffers from excessive numerical diffusion. The concept of artificial viscosity consists in modulating the effect of this dissipation by means of the parameter d. This coefficient may be $\theta(1)$ near discontinuities and $\theta(h^2)$ in the regions where the flow is "regular" to preserve the accuracy of the second-order scheme. Hence, at the discontinuities, the scheme is essentially the non oscillatory first-order scheme. Of course, the parameter d must be a function of a sensor which recognizes discontinuities in the flow.
We describe here two possible choices for the sensor.

1. Gradient of velocity

Consider the definition :

$$d_{j+\frac{1}{2}} = \chi \, 6\Delta t \, |\frac{\partial v}{\partial x}|_{j+\frac{1}{2}} \tag{13}$$

where $\frac{\partial v}{\partial x}$ is evaluated at the middle of the element $[j, j+1]$ and χ is an adjustable parameter.
Notice that $d_{j+\frac{1}{2}}$ is maximum inside shocks.

2. Second derivative of the pressure

Let us rather introduce the quantity

$$d_j = |\frac{p_{j+1} - 2p_j + p_{j-1}}{p_{j+1} + 2p_j + p_{j-1}}|$$

and define

$$d_{j+\frac{1}{2}} = \chi \; max(d_j, d_{j+1}) \tag{14}$$

Here the quantity $d_{j+\frac{1}{2}}$ is maximum on both sides of a shock but may vanish inside.

As shown in Fig.(2), when the parameter χ increases, the amplitude of oscillations is reduced and the shock's thickness increases in the case of the first sensor. On the contrary, Fig.(3) shows that, for the second sensor, the shock's thickness is less sensitive to variations of χ and the effect of dissipation is not so pronounced in the regular parts of the flow as it was in the case of the first sensor. Notice that the oscillations are rapidly damped using the two-step scheme(10) which gives generally a better overall accuracy than the one-step scheme(9).
The disadvantage of the artificial viscosity methods lies in that they introduce an adjustable parameter whose value is not always simple to determine. In the next sections parameter-free methods will be discussed.

IV. TVD methods

It is known[12] that the total variation

$$TV = \int_{-\infty}^{+\infty} |\frac{\partial u}{\partial x}| dx$$

of a solution of Eq.(3) can never increase. Correspondly, it seems desirable that the discrete total variation

$$TV = \sum_{j=-\infty}^{+\infty} |u_{j+1} - u_j|$$

of a solution of a discrete approximation to Eq.(3) should not increase. A discretization which has this property is said to be Total Variation Diminishing (TVD). Since the total variation will increase if an initially monotone profile ceases to be monotone, TVD schemes preserve monoticity.
We show here how to construct schemes endowed with such a property.

1. Upwind TVD method

1.1. *Scalar case*

Scheme(7) can be written in the form

$$u_j^{n+1} = u_j^n - \lambda(H_{j+\frac{1}{2}}^n - H_{j-\frac{1}{2}}^n) \tag{15}$$

where

$$H_{j+\frac{1}{2}} = \frac{1}{2}(f_j + f_{j+1} - \frac{1}{\lambda} q_{j+\frac{1}{2}} \Delta_{j+\frac{1}{2}} u_j)$$

and

$$q_{j+\frac{1}{2}} = \nu_{j+\frac{1}{2}}^2 + \frac{1}{3}$$

This scheme is TVD whenever the (sufficient) condition

$$|\nu_{j+\frac{1}{2}}| \leq q_{j+\frac{1}{2}} \leq 1$$

i.e.

$$|\nu_{j+\frac{1}{2}}| \leq \sqrt{\frac{2}{3}}$$

is fullfilled. Thus, it is TVD over the whole stability region. This scheme is however too much dissipative. Following Harten[4], we convert scheme(15) into a second-order accurate TVD scheme by applying it to an appropriately modified flux $f + \frac{1}{\lambda}g$. The resulting second-order accurate scheme is given by Eq.(15) :

$$u_j^{n+1} = u_j^n - \lambda(\tilde{H}_{j+\frac{1}{2}}^n - \tilde{H}_{j-\frac{1}{2}}^n) \tag{16}$$

with the modified flux

$$\lambda\tilde{H}_{j+\frac{1}{2}} = \frac{\lambda}{2}(f_j + f_{j+1}) + \frac{1}{2}(g_j + g_{j+1}) - \frac{1}{2}q(\nu_{j+\frac{1}{2}} + \gamma_{j+\frac{1}{2}})\Delta_{j+\frac{1}{2}}u_j$$

where

$$\gamma_{j+\frac{1}{2}} = \begin{cases} \Delta_{j+\frac{1}{2}}g_j/\Delta_{j+\frac{1}{2}}u_j & \text{if } \Delta_{j+\frac{1}{2}}u_j \neq 0 \\ 0 & \text{if } \Delta_{j+\frac{1}{2}}u_j = 0 \end{cases}$$

The anti-diffusive flux g approximates

$$h\,\sigma(\nu)\,\frac{\partial u}{\partial x}$$

where $\sigma(\nu) = \frac{1}{2}(q(\nu) - \nu^2) = \frac{1}{6}$ and thus cancels the first-order error.
Now the TVD condition becomes

$$|\nu_{j+\frac{1}{2}} + \gamma_{j+\frac{1}{2}}| \leq q(\nu_{j+\frac{1}{2}} + \gamma_{j+\frac{1}{2}}) \leq 1$$

i.e.

$$|\nu_{j+\frac{1}{2}}| \leq \sqrt{\frac{2}{3}} - |\gamma_{j+\frac{1}{2}}|$$

and the TVD interval is reduced. We can see that it is necessary to limit the flux g to ensure that $\gamma_{j+\frac{1}{2}}$ is bounded.
Examples of the limiter function g_j can be expressed as

$$g_j = \sigma\ s\ max[0,\ min(|\Delta_{j+\frac{1}{2}}u_j|, s\Delta_{j-\frac{1}{2}}u_j)] \tag{17}$$

for which $\gamma_{j+\frac{1}{2}} \leq \sigma \equiv \frac{1}{6}$;

$$g_j = \sigma\ s\ max[0,\ min(2|\Delta_{j+\frac{1}{2}}u_j|, s\Delta_{j-\frac{1}{2}}),\ min(|\Delta_{j+\frac{1}{2}}u_j|, 2s\Delta_{j-\frac{1}{2}}u_j)] \tag{18}$$

for which $\gamma_{j+\frac{1}{2}} \leq 2\sigma \equiv \frac{1}{3}$;

where s=sgn$(\Delta_{j+\frac{1}{2}}u_j)$.
The second limiter gives much sharper discontinuities than the first one but reduces the TVD interval (see Fig.(5)).

1.2. *Generalization to systems of equations*

Unlike in the scalar case, the total variation in x of the solution of a system of nonlinear conservation laws is not necessarily a monotonic decreasing function of time. The solution may actually increase at moments of interactions between the waves. Nevertheless, the scalar TVD scheme can be extended to a system of equations so that the resulting scheme is TVD for the "locally frozen" constant coefficients system. To accomplish this, we define at each point a "local" system of characteristic fields. We describe the above approach for hyperbolic systems of conservation laws such as (1).

Let $U_{j+\frac{1}{2}}$ be some convenient average of U_j and U_{j+1}, and let $a^l_{j+\frac{1}{2}}, T_{j+\frac{1}{2}}$ denote the quantities a^l, T evaluated at $U_{j+\frac{1}{2}}$. We define $\alpha^l_{j+\frac{1}{2}}$ as the component of $\Delta_{j+\frac{1}{2}}U_j$ in the lth characteristic direction, namely,

$$\Delta_{j+\frac{1}{2}}U_j = T_{j+\frac{1}{2}}\alpha_{j+\frac{1}{2}} \ ; \ \alpha_{j+\frac{1}{2}} = T^{-1}_{j+\frac{1}{2}}\Delta_{j+\frac{1}{2}}U_j \ . \tag{19}$$

With the above notations, scheme(16) can be applied scalarly to each of the locally defined characteristic variables of (1) as follows:

$$U^{n+1}_j = U^n_j - \lambda(\tilde{H}^n_{j+\frac{1}{2}} - \tilde{H}^n_{j-\frac{1}{2}}) \tag{20}$$

where

$$\lambda\tilde{H}_{j+\frac{1}{2}} = \frac{\lambda}{2}(F_j + F_{j+1}) + \frac{1}{2}T_{j+\frac{1}{2}}\Phi_{j+\frac{1}{2}} \tag{21}$$

$$\phi^l_{j+\frac{1}{2}} = g^l_j + g^l_{j+1} - q(\nu^l_{j+\frac{1}{2}} + \gamma^l_{j+\frac{1}{2}})\alpha^l_{j+\frac{1}{2}} \tag{22}$$

and $\nu^l_{j+\frac{1}{2}} = \lambda a^l_{j+\frac{1}{2}}$
As an example, limiter(17) becomes

$$g^l_j = \ \sigma \ s \ max[0, min(|\alpha^l_{j+\frac{1}{2}}|, s\alpha^l_{j-\frac{1}{2}})]$$

$$\gamma_{j+\frac{1}{2}} = \begin{cases} \Delta_{j+\frac{1}{2}}g^l_j/\alpha^l_{j+\frac{1}{2}} & \text{if } \alpha^l_{j+\frac{1}{2}} \neq 0 \\ 0 & \text{if } \alpha^l_{j+\frac{1}{2}} = 0 \end{cases}$$

where $s = sgn(\alpha^l_{j+\frac{1}{2}})$
The simplest form of $U_{j+\frac{1}{2}}$ is

$$U_{j+\frac{1}{2}} = \frac{1}{2}(U_{j+1} + U_j)$$

but we prefer to use Roe's averaging[13] that has the computational advantage of perfectly resolving stationary discontinuities (see also ref. [14] for a complete description of the procedure).

1.3. *Interpretations of the second-order TVD scheme*

We can give two interpretations of the second-order TVD scheme. We look at it
i) as a Lax-Wendroff scheme :

$$\lambda H^{LW}_{j+\frac{1}{2}} = \frac{\lambda}{2}(f_j + f_{j+1}) - \frac{\nu^2_{j+\frac{1}{2}}}{2}\Delta_{j+\frac{1}{2}}u_j \quad ,$$

to which is added an artificial viscosity term[15]

$$\lambda\tilde{H}_{j+\frac{1}{2}} = \lambda H^{LW}_{j+\frac{1}{2}} + \frac{1}{2}(g_j + g_{j+1}) - \frac{1}{2}[q(\nu_{j+\frac{1}{2}} + \gamma_{j+\frac{1}{2}}) - \nu^2_{j+\frac{1}{2}}]\Delta_{j+\frac{1}{2}}u_j$$

ii) as a first-order monotone scheme :

$$\lambda H_{j+\frac{1}{2}} = \frac{\lambda}{2}(f_j + f_{j+1}) - \frac{1}{2}q(\nu_{j+\frac{1}{2}})\Delta_{j+\frac{1}{2}}u_j,$$

with an added antidiffusion term[6]

$$\lambda\tilde{H}_{j+\frac{1}{2}} = \lambda H_{j+\frac{1}{2}} + \frac{1}{2}(g_j + g_{j+1}) - \frac{1}{2}[q(\nu_{j+\frac{1}{2}} + \gamma_{j+\frac{1}{2}}) - q(\nu_{j+\frac{1}{2}})]\Delta_{j+\frac{1}{2}}u_j$$

These two interpretations will lead to methods described in the next sections : symmetric TVD methods and FCT methods (or antidiffusion methods).

REMARK : For systems of equations, the scheme is constructed using these interpretations. In fact, the only term for which the implementation uses the decomposition along the characteristics is the artificial viscosity one.

2. Symmetric TVD methods

Following the last interpretation, we can obtain other second-order TVD schemes. The strategy is

i)to locate the regions where the second-order accurate scheme produces oscillations,
ii)to introduce there the maximum dissipation($\rightarrow$ monotone scheme),
iii)to reduce or to compensate the dissipation in the other parts of the flow .

We describe now two ways to achieve this strategy.

2.1. *Flux limiter TVD method*

In this method, the artificial viscosity term $d_{j+\frac{1}{2}}$ (see II.3) is evaluated using the variations of a sensor w over three contiguous elements : $\Delta_{j-\frac{1}{2}}w_j$, $\Delta_{j+\frac{1}{2}}w_j$ and $\Delta_{j+\frac{3}{2}}w_j$.
Denote by r^+ and r^- the ratios :

$$r^+ = \frac{\Delta_{j+\frac{3}{2}}w_j}{\Delta_{j+\frac{1}{2}}w_j} \; ; \; r^- = \frac{\Delta_{j+\frac{1}{2}}w_j}{\Delta_{j-\frac{1}{2}}w_j}$$

we define

$$d_{j+\frac{1}{2}} = \begin{cases} 0 & \text{if } r^+ < 0 \text{ or } r^- < 0 \ (extremum) \\ \text{1-B}(r_s^+, r_s^-) & \text{otherwise} \end{cases} \tag{23}$$

where

$$r_s^+ = \frac{min(|\Delta_{j+\frac{1}{2}}w_j|, |\Delta_{j+\frac{3}{2}}w_j|)}{max(|\Delta_{j+\frac{1}{2}}w_j|, |\Delta_{j+\frac{3}{2}}w_j|)}$$

$$r_s^- = \frac{min(|\Delta_{j-\frac{1}{2}}w_j|, |\Delta_{j+\frac{1}{2}}w_j|)}{max(|\Delta_{j-\frac{1}{2}}w_j|, |\Delta_{j+\frac{1}{2}}w_j|)}$$

and $B(r_s^+, r_s^-) = min[B(r_s^+), B(r_s^-)]$.
The function $B(r)$ is a limiter function that takes values in the interval $[0, 1]$. Some examples are

$$B(r) = \; min(\frac{2r}{1+r}, 1) \quad (\ van\ Leer\ ) \tag{24}$$

$$B(r) = \; min(2r, 1) \quad (\ Roe's\ superbee\ ) \tag{25}$$

We note in passing that other definitions of $r^{\pm}$ have been proposed, among others, by Sweby[5] and Davis[15] .

If the conservative variables are choosen as sensor, the solution presents low frequency oscillations. A better choice is to take a unique sensor for the whole system of equations, so that the dissipation coefficient is the same for all the equations. In the examples illustrated in Fig.(6), the sensor is the Mach number($M = \frac{v}{c}$) which is very sensitive to oscillations.

2.2. *Characteristic TVD method*

An other possibility is to work with the characteristic variables. Following Yee[16], the variations $\Delta_{j+\frac{1}{2}} U_j$ is decomposed into the components $\alpha^l_{j+\frac{1}{2}}$ in the lth characteristic direction.
The artificial dissipation term(12) is written in the following form

$$D_{j+\frac{1}{2}} U_j = T_{j+\frac{1}{2}} \Psi_{j+\frac{1}{2}} \tag{26}$$

where

$$\psi^l_{j+\frac{1}{2}} = \frac{1}{6}[\alpha^l_{j+\frac{1}{2}} - \hat{Q}^l_{j+\frac{1}{2}}] \tag{27}$$

and $\hat{Q}^l_{j+\frac{1}{2}}$ is a limiter function.
Some examples of such a function are

$$\begin{aligned}
(a) \quad & \hat{Q}^l_{j+\frac{1}{2}} = minmod(\alpha^l_{j-\frac{1}{2}}, \alpha^l_{j+\frac{1}{2}}, \alpha^l_{j+\frac{3}{2}}) \\
(b) \quad & \hat{Q}^l_{j+\frac{1}{2}} = minmod(2\alpha^l_{j-\frac{1}{2}}, 2\alpha^l_{j+\frac{1}{2}}, 2\alpha^l_{j+\frac{3}{2}}, \frac{1}{2}(\alpha^l_{j-\frac{1}{2}} + \alpha^l_{j+\frac{3}{2}})) \\
(c) \quad & \hat{Q}^l_{j+\frac{1}{2}} = minmod(6\alpha^l_{j-\frac{1}{2}}, \alpha^l_{j+\frac{1}{2}}, 6\alpha^l_{j+\frac{3}{2}})
\end{aligned} \tag{28}$$

The minmod function of a list of arguments is equal to the smallest number in absolute value if the arguments are of the same sign, or is equal to zero if any two arguments are of opposite sign.
Fig.(7) illustrates the effect of the different limiters on the accuracy of the numerical solution.

V. FCT methods

It has been noticed that the first-order scheme can be regarded as a discretized version of a parabolic equation of the form

$$\frac{\partial u}{\partial t} + \frac{\partial f}{\partial x} = \frac{h^2}{6\Delta t}\frac{\partial^2 u}{\partial x^2}$$

where $\frac{h^2}{6\Delta t}$ is the coefficient of the diffusion term.
The basis of the Flux Corrected Transport(FCT) method or antidiffusion method is to use a modification of the diffusive scheme to remove the diffusion in the regular part of the flow and to limit it near discontinuities in such a way as to prevent the formation of new extrema.

1. Antidiffusion methods

In the method of Boris and Book[6], one can introduce the antidiffusion term by operator splitting. The procedure is as follows :

$$\begin{aligned} u_j^{n+\frac{1}{2}} &= u_j^n - \lambda(H_{j+\frac{1}{2}}^n - H_{j-\frac{1}{2}}^n) \\ u_j^{n+1} &= u_j^{n+\frac{1}{2}} - (D_{j+\frac{1}{2}}^c - D_{j-\frac{1}{2}}^c)u_j^{n+\frac{1}{2}} \end{aligned} \tag{29}$$

where $D_{j+\frac{1}{2}}^c u_j$ is a corrected flux defined here by

$$D_{j+\frac{1}{2}}^c u_j = s\ max[0,\ min(s\Delta_{j-\frac{1}{2}}u_j, \frac{1}{6}|\Delta_{j+\frac{1}{2}}u_j|, s\Delta_{j+\frac{3}{2}}u_j)] \tag{30}$$

where $s = sgn(\Delta_{j+\frac{1}{2}}u_j)$.
Notice that the second step of this procedure is nothing but an approximation of the backward heat equation. This scheme allows very sharp discontinuities, but does not eliminate oscillations of low frequency. As we have shown previously, a better choice is to work with the locally frozen characteristic variables.
In this case, the corrected flux can be written as

$$D_{j+\frac{1}{2}}^c U_j = T_{j+\frac{1}{2}}\Psi_{j+\frac{1}{2}} \tag{31}$$

where

$$\psi^l_{j+\frac{1}{2}} = s\ max[0,\ min(s\alpha^l_{j-\frac{1}{2}}, \frac{1}{6}|\alpha^l_{j+\frac{1}{2}}|, s\alpha^l_{j+\frac{3}{2}})] \tag{32}$$

and $s = sgn(\alpha^l_{j+\frac{1}{2}})$.
The solution obtained with this scheme is not devoid of a little undershoot behind the shock. This undershoot can be eliminated using a much dissipative limiter such as (28.*b*) for example.

Finally, an other way to construct the antidiffusion flux is to use the artificial compression method of Harten[17,18].
In this method, $\psi^l_{j+\frac{1}{2}}$ is defined by

$$\psi^l_{j+\frac{1}{2}} = (g^l_{j+1} + g^l_j) - |\gamma^l_{j+\frac{1}{2}}|\alpha^l_{j+\frac{1}{2}} \tag{33}$$

where g^l_j is a limiter function such as (18) and

$$\gamma_{j+\frac{1}{2}} = \begin{cases} \Delta_{j+\frac{1}{2}} g^l_j / \alpha^l_{j+\frac{1}{2}} & \text{if } \alpha^l_{j+\frac{1}{2}} \neq 0 \\ 0 & \text{if } \alpha^l_{j+\frac{1}{2}} = 0 \end{cases}$$

This schemes are illustrated in Fig.(8).

2. Zalesak's method

An other method for constructing FCT schemes has been proposed by Zalesak[19]. If we note that first-order and second-order schemes can be expressed in the form

$$u^{n+1}_j = u^n_j - \lambda(ft_{j+\frac{1}{2}} - ft_{j-\frac{1}{2}})$$

where $ft_{j+\frac{1}{2}}$ are called transportive fluxes, the procedure is described in the following way :

(1) Compute $ft^L_{j+\frac{1}{2}}$, the transportive flux given by the low order scheme
(2) Compute $ft^H_{j+\frac{1}{2}}$, the transportive flux given by the high order scheme
(3) Define the "antidiffusive flux"

$$at_{j+\frac{1}{2}} = ft^H_{j+\frac{1}{2}} - ft^L_{j+\frac{1}{2}}$$

(4) Compute the update low order("transported and diffused") solution :

$$u^{td}_j = u^n_j - \lambda(ft^L_{j+\frac{1}{2}} - ft^L_{j-\frac{1}{2}})$$

(5) Limit $at_{j+\frac{1}{2}}$ in such a manner that u^{n+1} as computed in the sixth step below will contain no extrema apart those found in u^{td} and u^n :

$$at^c_{j+\frac{1}{2}} = l_{j+\frac{1}{2}}\ at_{j+\frac{1}{2}}\ ;\ 0 \leq l_{j+\frac{1}{2}} \leq 1$$

(6) Apply the limited antidiffusive fluxes :

$$u^{n+1}_j = u^{td}_j - \lambda(at^c_{j+\frac{1}{2}} - at^c_{j-\frac{1}{2}})$$

Clearly for $l = 1$ in step 5, the usual oscillatory solution will be obtained and thus the selection of limiters is crucial in the construction of FCT schemes. We recall here the FCT limiter presented in the paper of Zalesak.

For each node j, we define

$$P^+_j = max(0, \lambda\ at_{j-\frac{1}{2}}) - min(0, \lambda\ at_{j+\frac{1}{2}})$$
$$Q^+_j = u^{max}_j - u^{td}_j$$
$$R^+_j = \begin{cases} \min(1, Q^+_j/P^+_j) & \text{if } P^+_j > 0 \\ 0 & \text{if } P^+_j = 0 \end{cases}$$

and similarly

$$P^-_j = max(0, \lambda\ at_{j+\frac{1}{2}}) - min(0, \lambda\ at_{j-\frac{1}{2}})$$
$$Q^-_j = u^{td}_j - u^{min}_j$$
$$R^-_j = \begin{cases} \min(1, Q^-_j/P^-_j) & \text{if } P^-_j > 0 \\ 0 & \text{if } P^-_j = 0 \end{cases}$$

We have choosen the quantities $l_{j+\frac{1}{2}}$, u^{max}_j and u^{min}_j as

$$l_{j+\frac{1}{2}} = min(R^+_j, R^-_j, R^+_{j+1}, R^-_{j+1})$$
$$u^{max}_j = max(u^a_{j-1}, u^a_j, u^a_{j+1})$$
$$u^{min}_j = min(u^b_{j-1}, u^b_j, u^b_{j+1})$$

where $u^a_j = max(u^n_j, u^{td}_j)$ and $u^b_j = min(u^n_j, u^{td}_j)$. But other choices are possible[19,20].

The extension of the above method to the solution of a system of equations as the Euler equations is not obvious. We mention the choice

$$l^1_{j+\frac{1}{2}} = min(l^\rho_{j+\frac{1}{2}}, l^e_{j+\frac{1}{2}}) \qquad (34)$$

$$l^2_{j+\frac{1}{2}} = min(l^\rho_{j+\frac{1}{2}}, l^m_{j+\frac{1}{2}}, l^e_{j+\frac{1}{2}}) \tag{35}$$

where l^ρ, l^m and l^e are the limiters constructed for each conservative variable[21].

In the problem of Sod, the resolution of shocks is quite good for the two limiters, but too much dissipation is present in the rarefaction wave and in the contact discontinuity for the second limiter (see Fig.(9)).

VI. Conclusion

In this report we have compared different techniques to construct non-oscillatory second-order shock-capturing schemes. The artificial viscosity methods appear to be the least diffusive in the regular part of the flow but introduce a parameter which is not always easy to evaluate. On the other hand, TVD and FCT methods have not this disavantage but the quality of the solution depends on the choice of the limiter function. Moreover, these schemes often add dissipation in the smooth region of the flow.

In general, we think that the artificial viscosity methods must be used as long as there is no very strong shocks in the flow. In the opposite case, the TVD and FCT methods give much more robust schemes. A report concerning the generalization of these techniques in a finite element multidimensional context is in preparation.

VII. References

[1] J. DONEA, A Taylor-Galerkin Method for Convective Transport Problems; Internat. J. Numer. Meths. Engrg. 20(1984) 101-120 .

[2] J. von NEUMANN and R.D. RICHTMYER, A Method for the Numerical Calculation of Hydrodynamic Shocks; J. Appl. Phys. 21(1950) 232-237 .

[3] A. LAPIDUS, A Detached Shock Calculation by Second-Order Finite Differences; J. Comput. Phys. 2(1967) 154-177 .

[4] A. HARTEN, On a Class of High Resolution Total-Variation-Stable Finite-Difference Schemes; NYU Report, October 1982 .

[5] P.K. SWEBY, High Resolution Schemes Using Flux Limiters for Hyperbolic Conservation Laws; SIAM J. Num. Anal. 21(1984) 995-1011 .

[6] J.P. BORIS and D.L. BOOK, Flux Corrected Transport, I. SHASTA, A Fluid Transport Algorithm That Works; J. Comput. Phys. 11(1973) 38-69 .

[7] G.A. SOD, A Survey of Several Finite Difference Methods for Systems of Nonlinear Hyperbolic Conservation Laws; J. Comput. Phys. 27(1978) 1-31 .

[8] P.D. LAX and B. WENDROFF, Difference Schemes for Hyperbolic Equations with High Order of Accuracy; Comm. Pure Appl. Math. 17(1964) .

[9] J. DONEA, L. QUARTAPELLE and V. SELMIN, An Analysis of Time Discretization in the Finite Element Solution of Hyperbolic Problems; to be published in J. Comput. Phys. (1987) .

[10] V. SELMIN, Solution by a Finite Element Method of Hyperbolic Problems with Discontinuities; Ph.D. Thesis, University of Liège, 1985-86

[11] A. HARTEN, J. HYMAN and P. LAX, On Finite-Difference Approximations and Entropy Conditions for Shocks; Comm. Pure Appl. Math. 29(1976) 297-322 .

[12] P.D. LAX, Hyperbolic Systems of Conservation Laws and the Mathematical Theory of Shock Waves; SIAM Regional Series on Applied Mathematics 11(1973) .

[13] P.L. ROE, Approximate Riemann Solvers, Parameter Vectors, and Difference Schemes; J. Comput. Phys. 43(1981) 357-372 .

[14] H.C. YEE, R.F. WARMING and A.HARTEN, Implicit Total Variation Diminishing(TVD) Schemes for Steady-State Calculations; AIAA Paper 83-1902 .

[15] S.F. DAVIS, TVD Finite Difference Schemes and Artificial Viscosity; ICASE Report 84-53 .

[16] H. C. YEE, Numerical Experiments with a Symmetric High-Resolution Shock-Capturing Scheme; NASA TM 88325 .

[17] A. HARTEN, The Artificial Compression Method for Computation of Shocks and Contact Discontinuities: III. Self-Adjusting Hybrid Schemes; Math. Comp. 32(1978) 363-389 .

[18] A. HARTEN, Adaptative Numerical Methods for Hyperbolic Conservation Laws; in Proc. of the Workshop on Adaptive Numerical Methods for Partial Differential Equations, University of Maryland, February 1983 .

[19] S.T. ZALESAK, Fully Multidimensional Flux-Corrected Transport Algorithms for Fluids; J. Comput. Phys. 31(1979) 335-362 .

[20] A.K. PARROTT and M.A. CHRISTIE, FCT Applied to the 2-D Finite Element Solution of Tracer Transport by a Single Phase Flow in a Porous Medium; in Proc. of the ICFD Conference on Numerical Methods for Fluid Dynamics, Reading, April 1985 .

[21] K. MORGAN, R. LOEHNER, J.R. JONES, J.PERAIRE and M. VAHDATI , Finite Element FCT for the Euler and Navier-Stokes Equations; in Proc. 6th Int. Symp. Finite Element Methods in Flow Problems, INRIA (1986) .

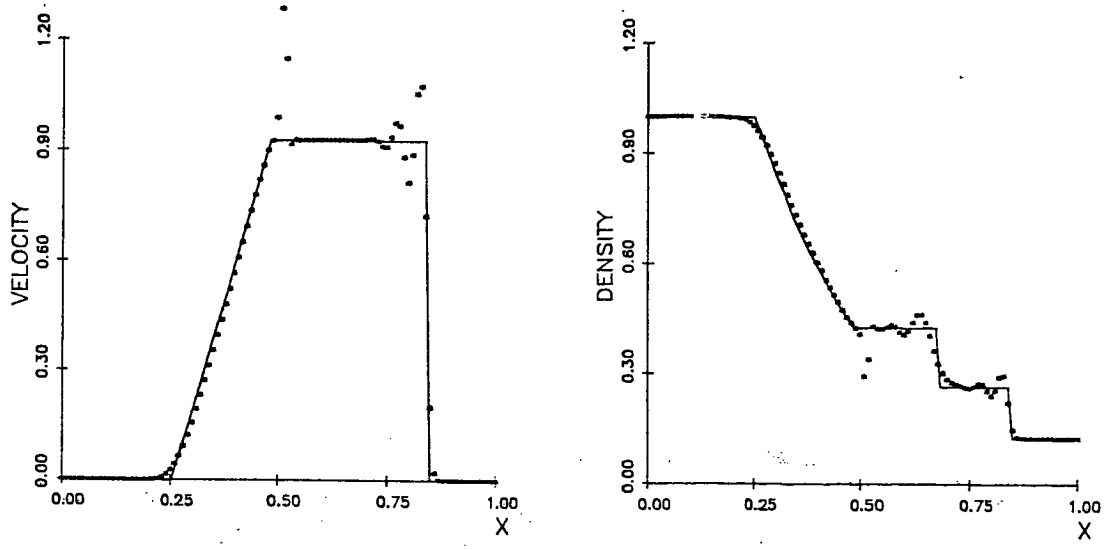

Lax-Wendroff finite difference scheme .

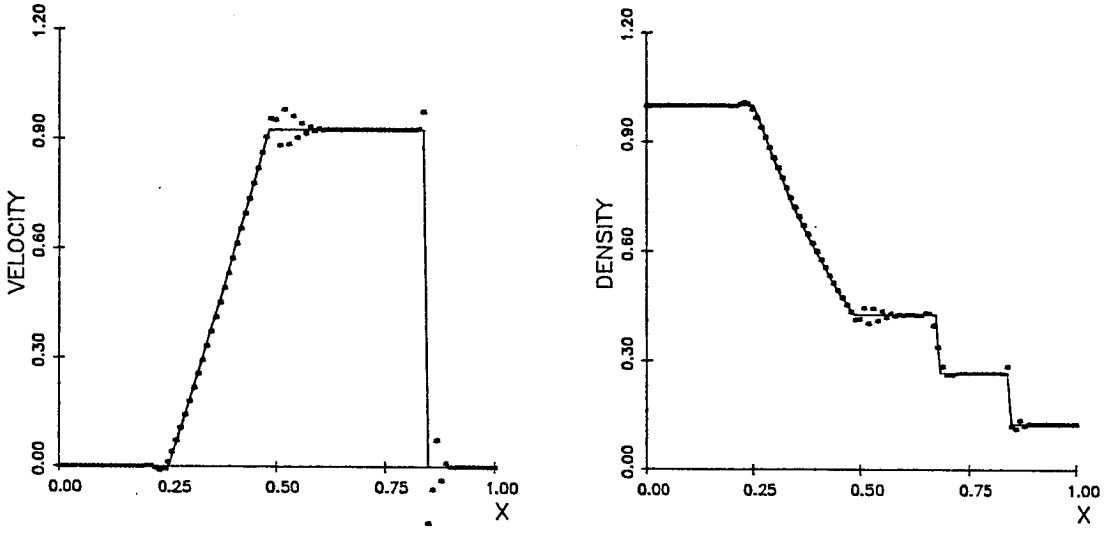

Lax-Wendroff finite element scheme .

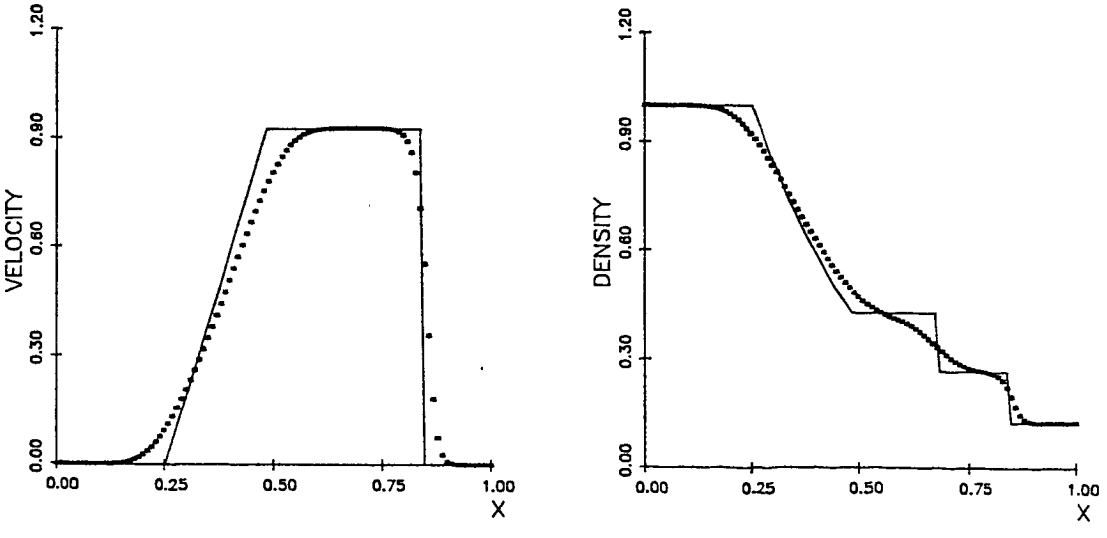

First-order scheme .

Fig. 1 . First- and second-order schemes ($\nu = 0.55$) .

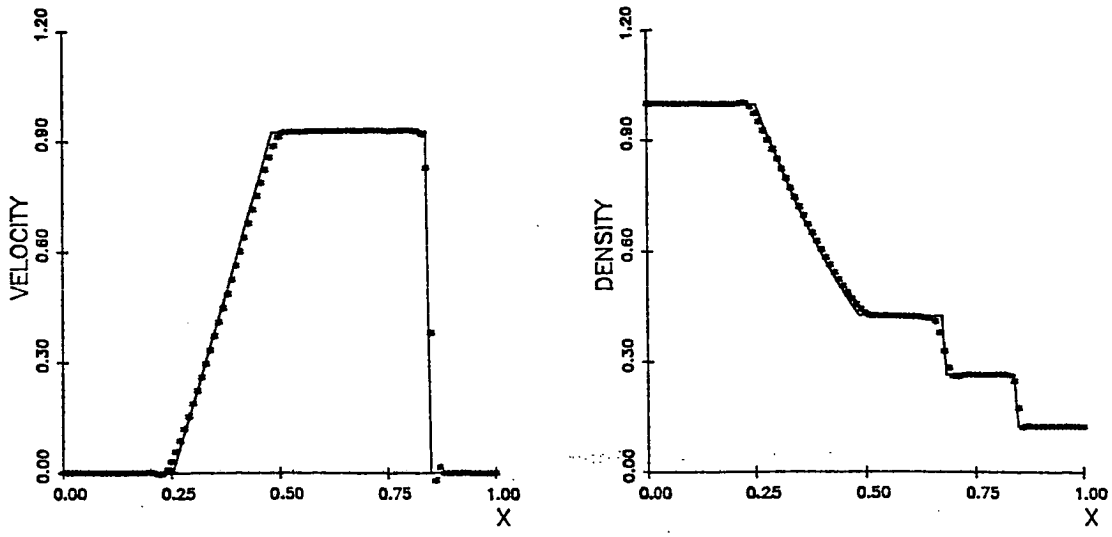

Two-step scheme ; $\chi = 0.5$.

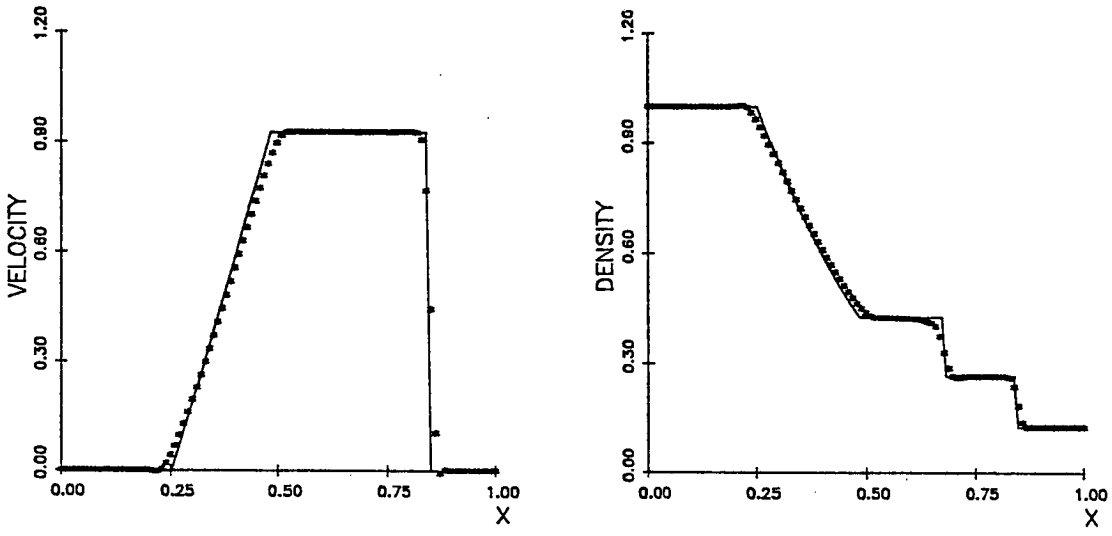

Two-step scheme ; $\chi = 1.0$.

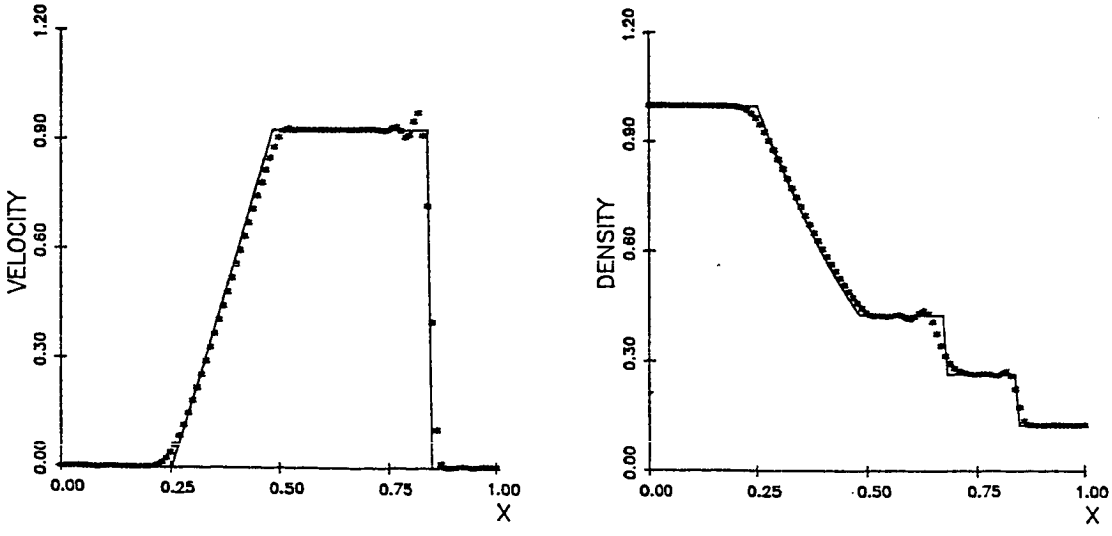

One-step scheme ; $\chi = 1.0$.

Fig. 2 . Artificial viscosity method ($\nu = 0.55$). Sensor : gradient of the velocity

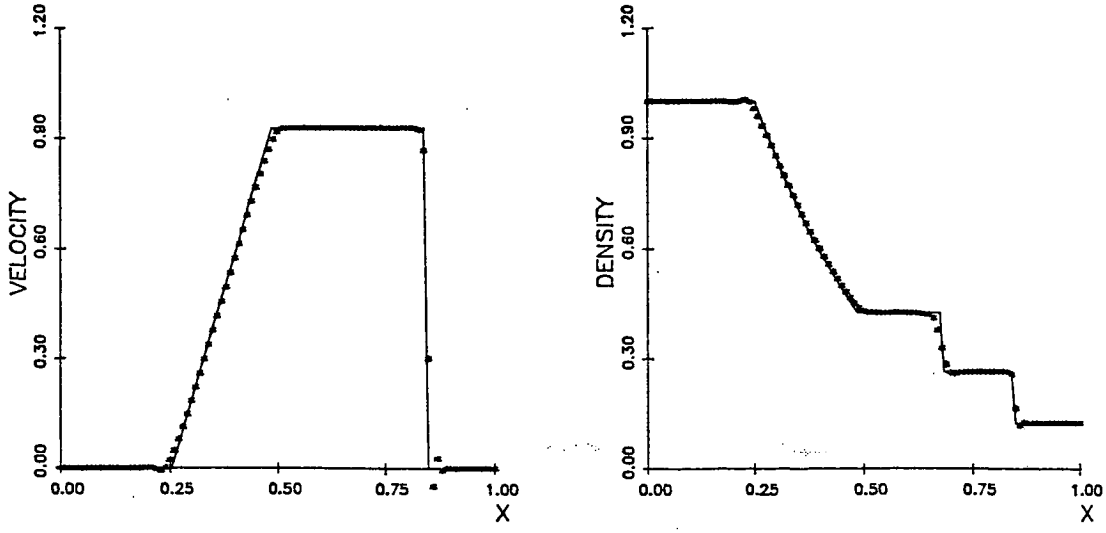

Two-step scheme ; $\chi = 1.5$.

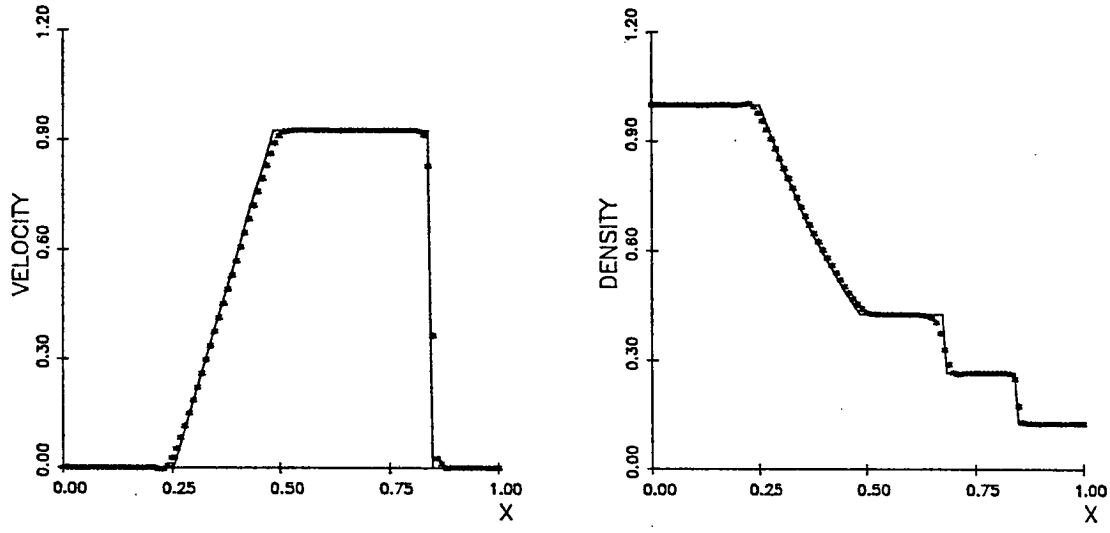

Two-step scheme ; $\chi = 3.0$.

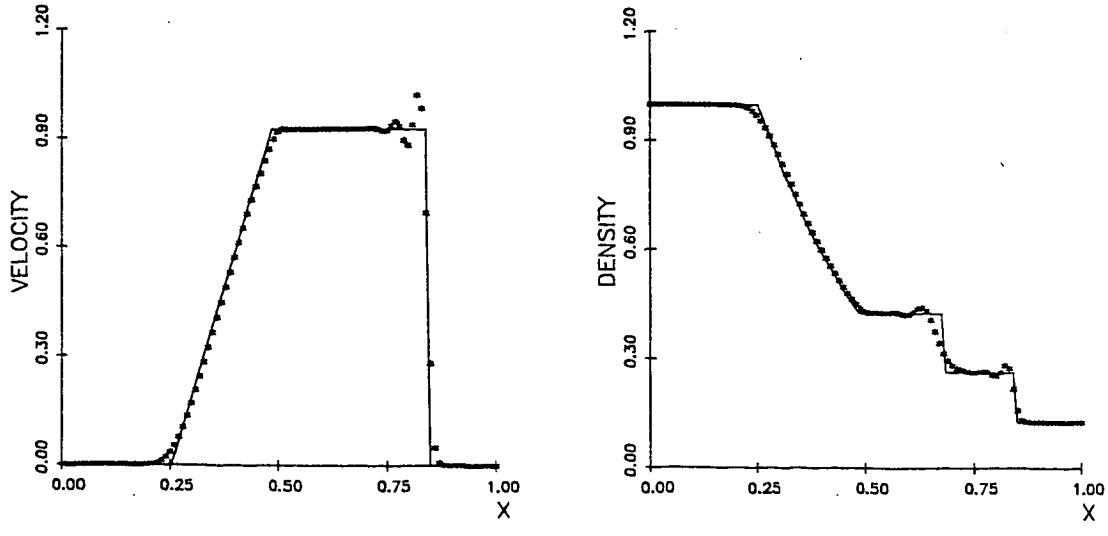

One-step scheme ; $\chi = 3.0$.

Fig. 3 . Artificial viscosity method ($\nu = 0.55$). Sensor : second derivative of the pressure .

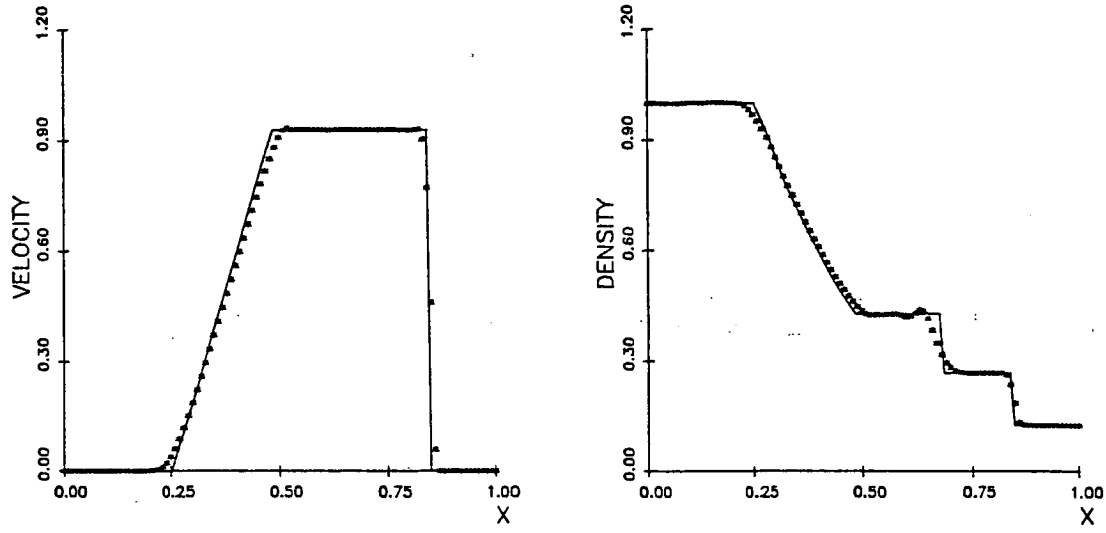

Sensor : gradient of the velocity ; $\chi = 1.0$.

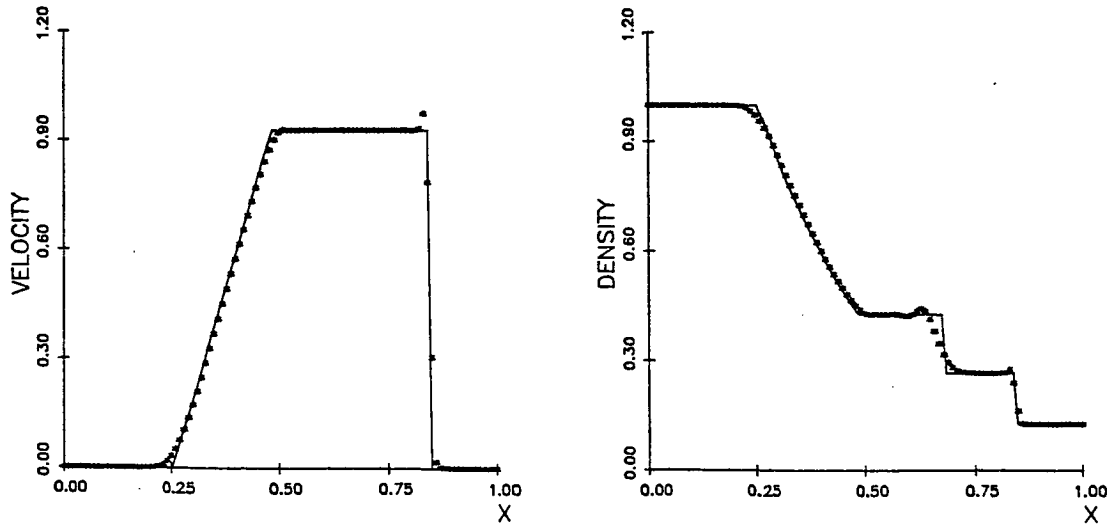

Sensor : second derivative of the pressure ; $\chi = 3.0$.

Fig. 4 . Artificial viscosity method ($\nu = 0.916$). One-step scheme .

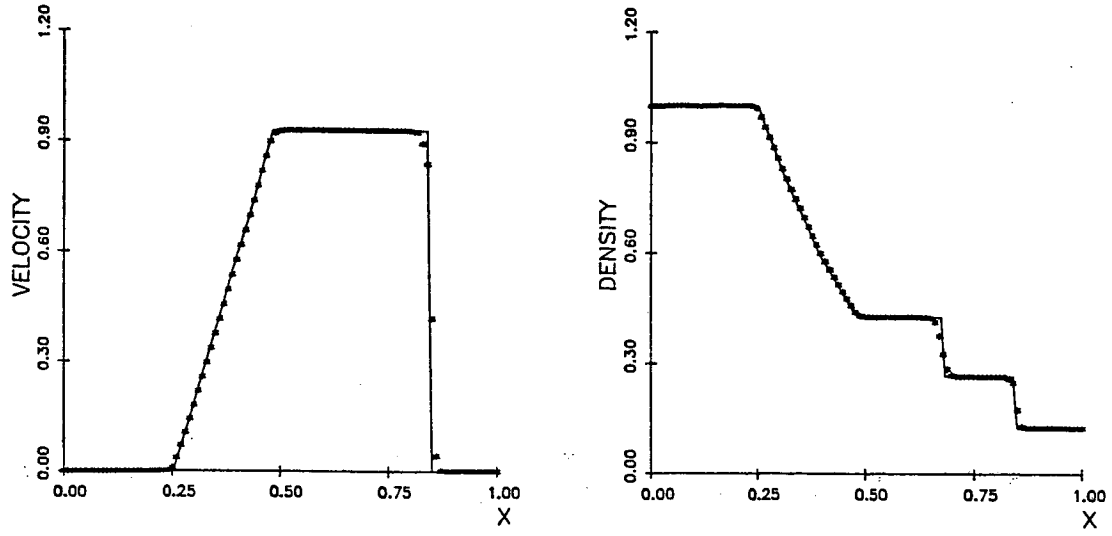

Limiter function (18) ; $\nu = 0.55$.

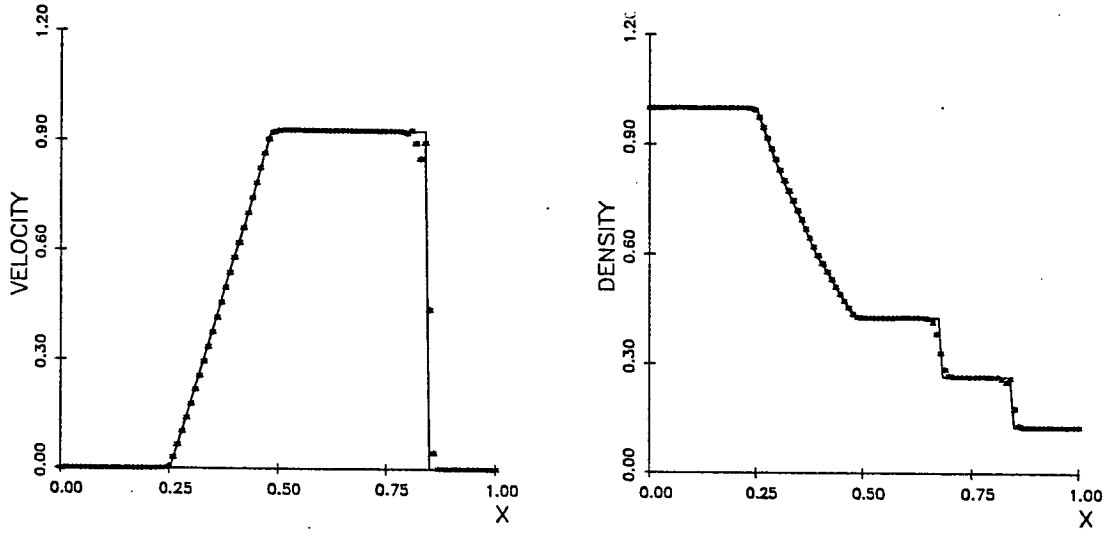

Limiter function (18) ; $\nu = 0.733$.

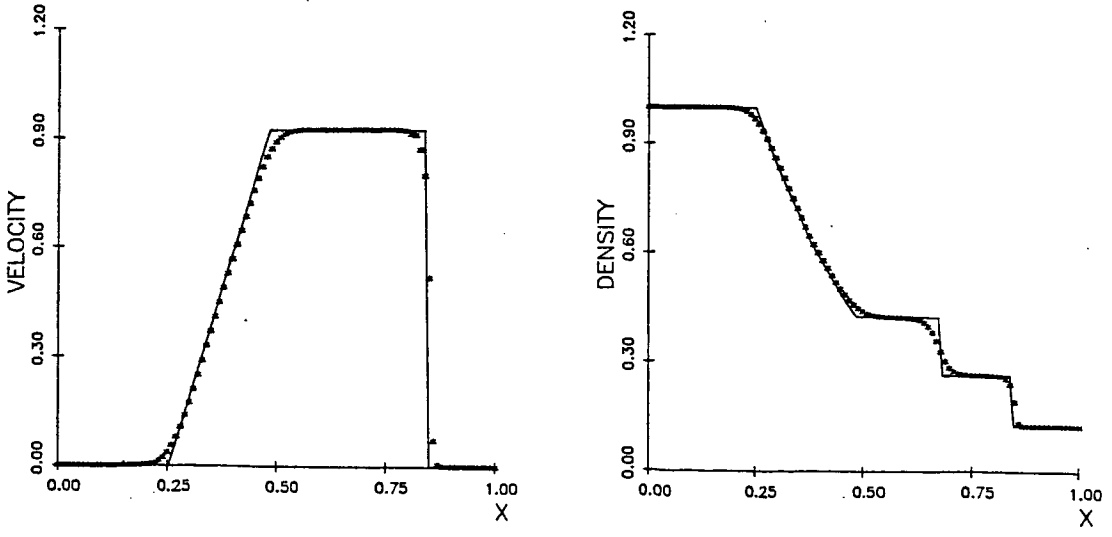

Limiter function (17) ; $\nu = 0.733$.

Fig. 5 . Upwind TVD method .

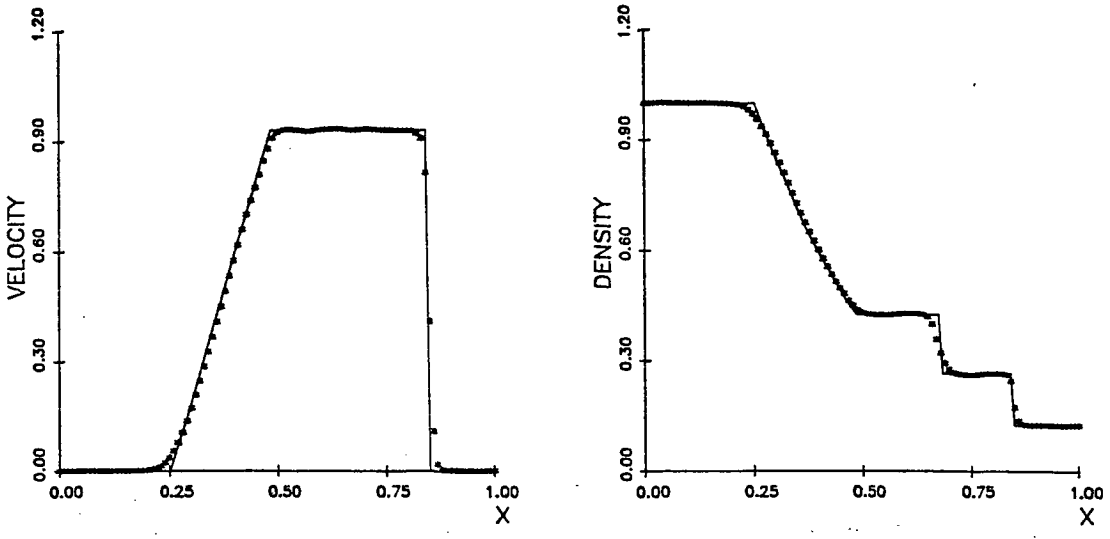

One-step scheme ($\nu = 0.733$). Sensor : conservative variables .

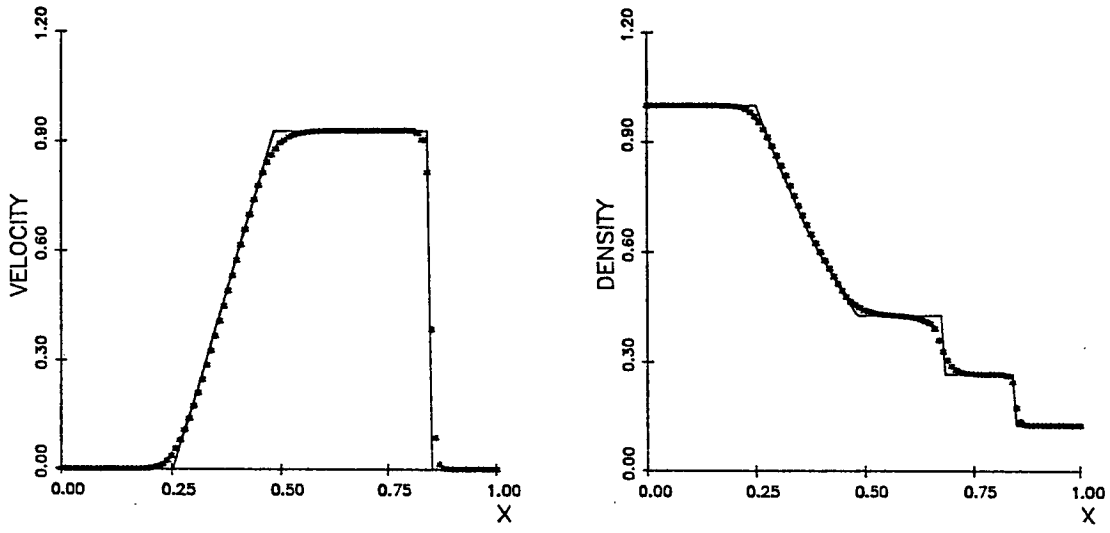

One-step scheme ($\nu = 0.733$). Sensor : Mach number .

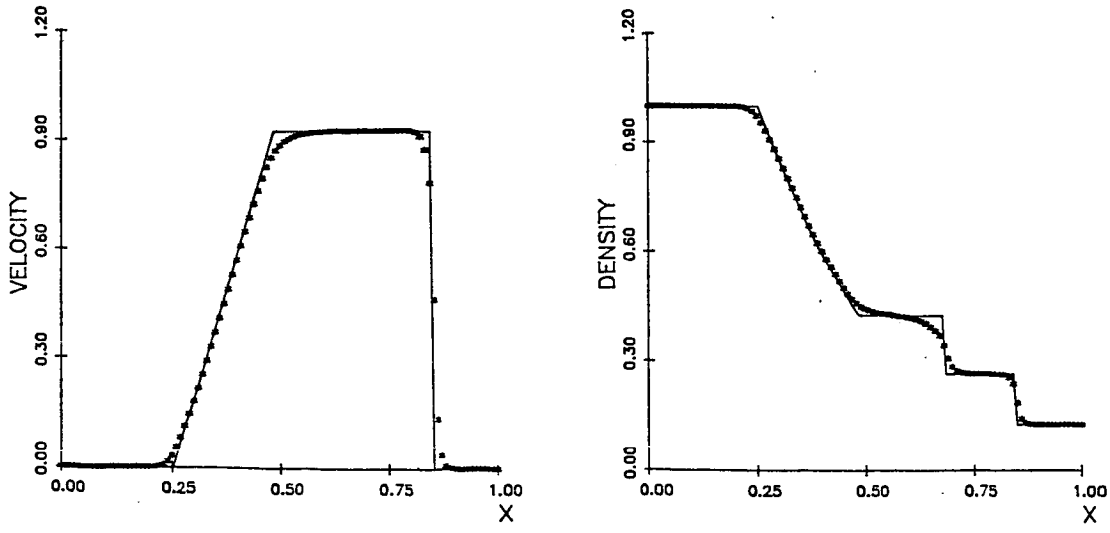

Two-step scheme ($\nu = 0.55$). Sensor : Mach number .

Fig. 6 . Flux limiter TVD method. Limiter function (25) .

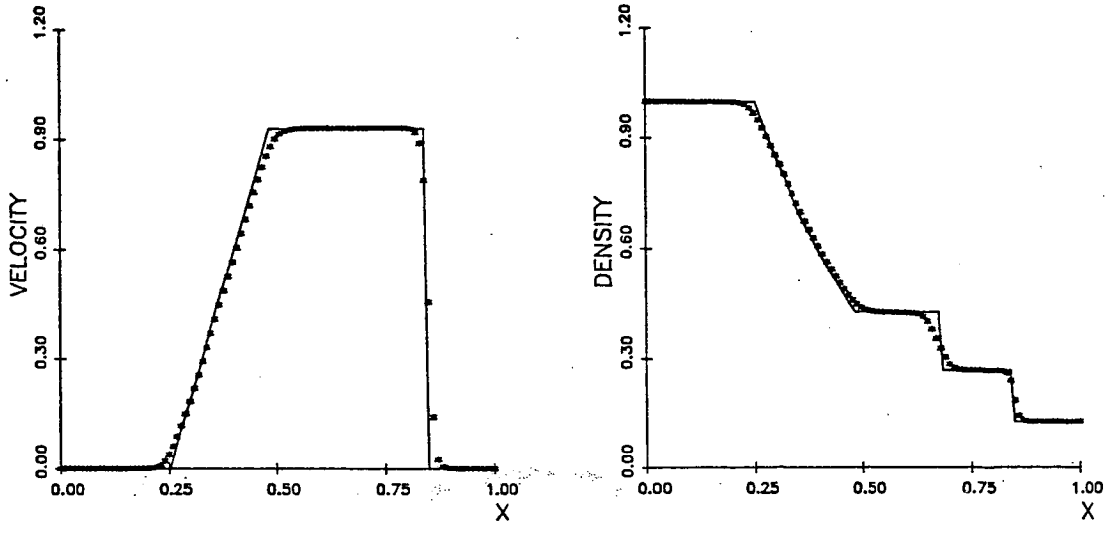

Two-step scheme ($\nu = 0.55$). Limiter function (28.b) .

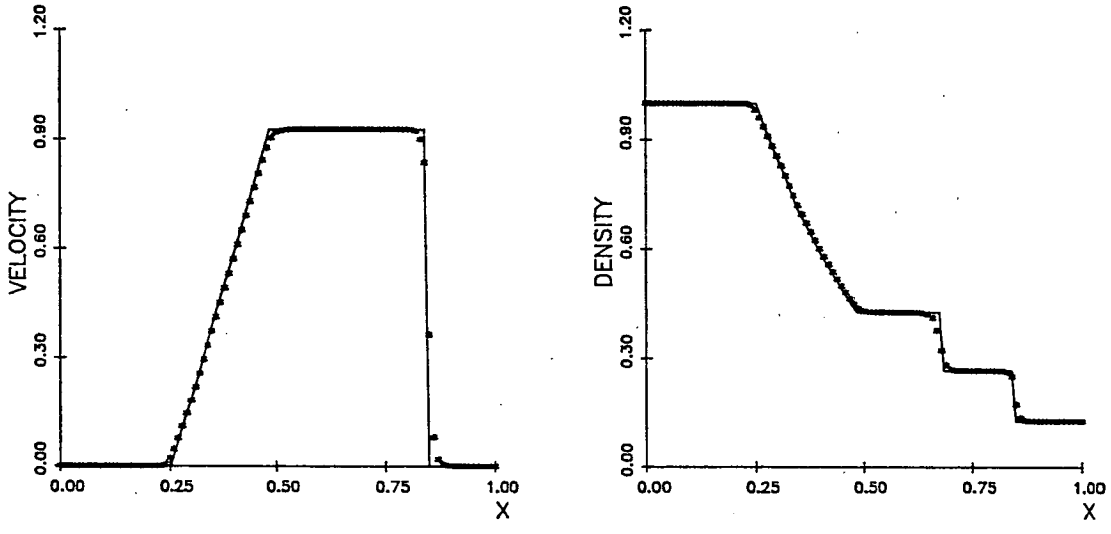

Two-step scheme ($\nu = 0.55$). Limiter function (28.c) .

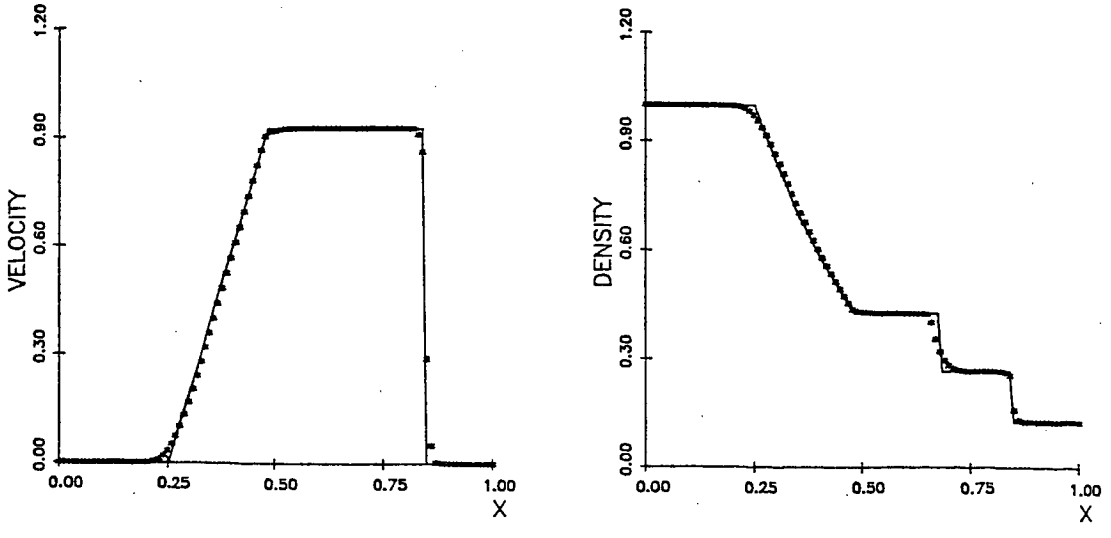

One-step scheme ($\nu = 0.733$). Limiter function (28.c) .

Fig. 7 . Characteristic TVD method .

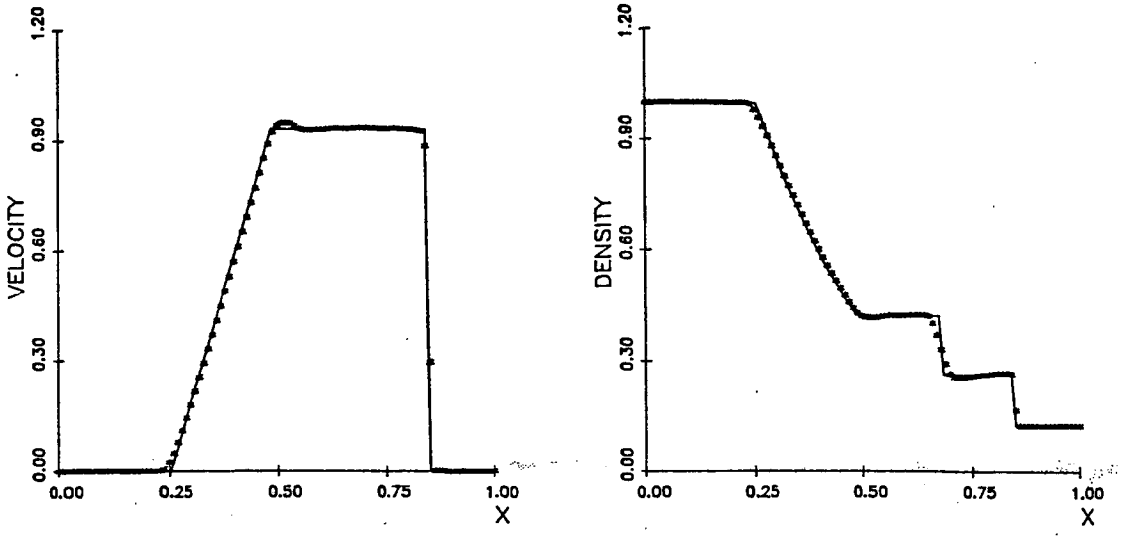

Boris and Book method ; conservative variables .

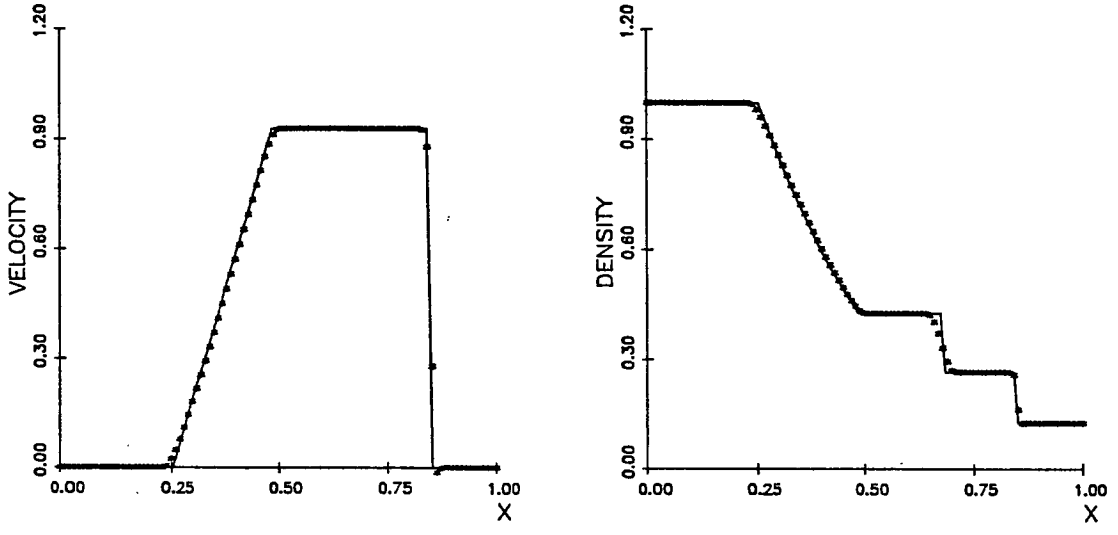

Boris and Book method ; characteristic variables .

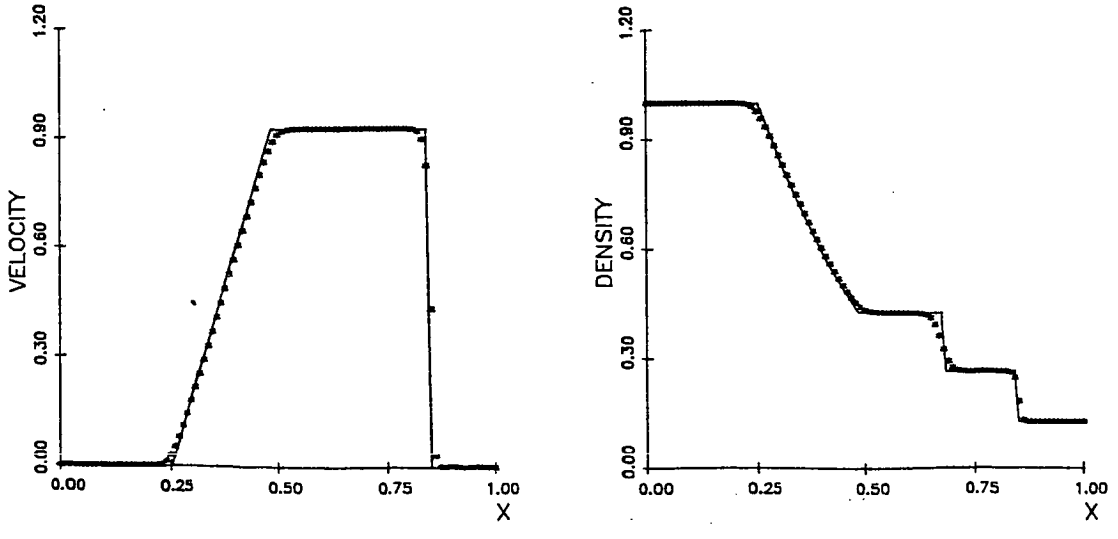

Artificial compression method .

Fig. 8 . Antidiffusion methods ($\nu = 0.733$) .

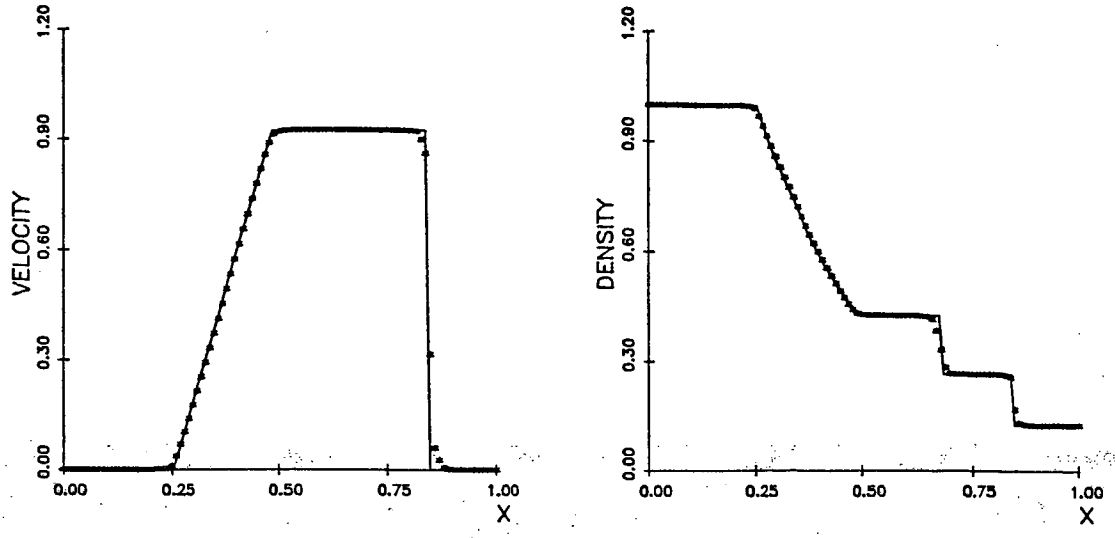

Two-step scheme ($\nu = 0.55$). Limiter function (34) .

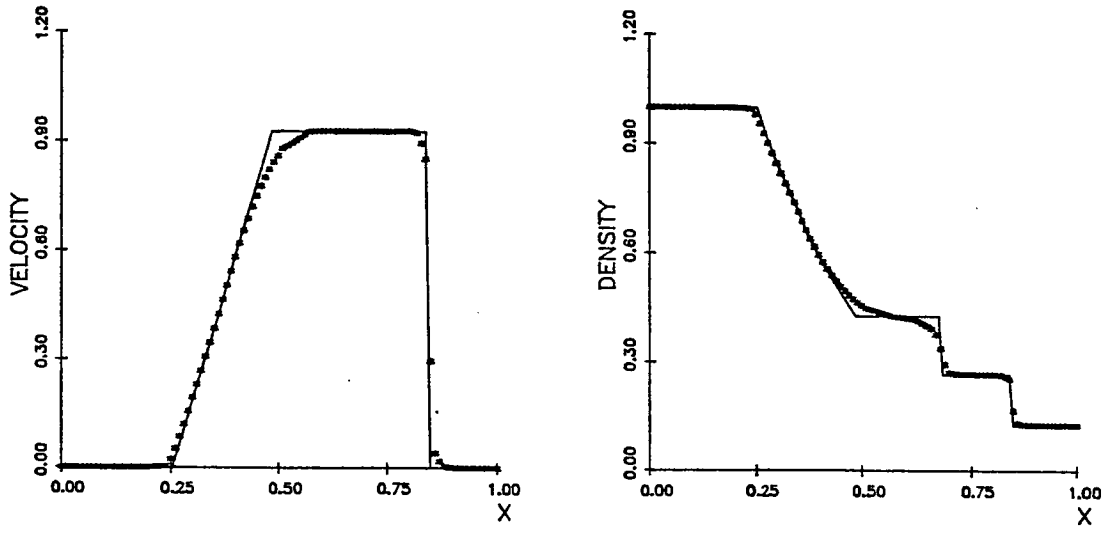

Two-step scheme ($\nu = 0.55$). Limiter function (35) .

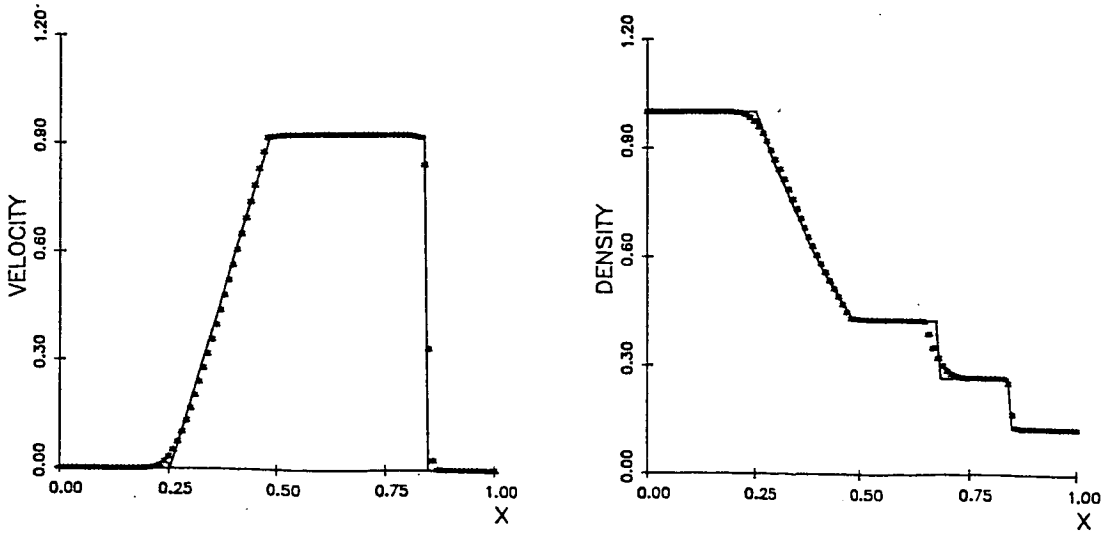

One-step scheme ($\nu = 0.733$). Limiter function (34) .

Fig. 9 . Zalesak's method .